JOURNAL OF ELECTROMAGNETIC ENGINEERING AND SCIENCE, VOL. 22, NO. 2, 138~145, MAR. 2022

https://doi.org/10.26866/jees.2022.2.r.70
ISSN 2671-7263 (Online) · ISSN 2671-7255 (Print)

Design and Analysis of a Compact GSM/GPS Dual-Band Bandpass Filter Using a T-Shaped Resonator

Abdul Basit[1,*] · Muhammad Irfan Khattak[1] · Mauth Al-Hasan[2] · Jamel Nebhen[3] · Atif Jan[1]

Abstract

This study presents an ultracompact dual-band bandpass filter with controllable transmission zeros based on quarter-wave dual-mode resonator for GSM (global system for mobile communications) and GPS (global positioning system) wireless applications. The filter is made up of two quarter-wave resonators, which help to independently control the passbands. A direct feed resonator creates the first operating band, which serves as a feeding source for the interior resonator and operates at a higher frequency band. Therefore, a pair of transmission zeros can be energized between the two passbands, and high roll-off skirts are obtained. To reduce the size of the entire filter, the two resonators are bent and connected together through a hole in a metal base. The structure is symmetrical in nature, so both frequency bands can be obtained using the even-odd mode analysis method. For GSM applications, the center frequency of the first working band is 850 MHz, while for GPS wireless applications, the center frequency of the second working band is 1.57 GHz. Although there is a feed line (λ_g is based on a waveguide length of 850 MHz), the filter has been simulated and fabricated for verification, with an ultra-compact size of 0.10 $\lambda_g \times 0.09\ \lambda_g$ (0.0095 λ_g^2). The simulation results and measured results match well, and the theory of the design concept is recognized.

Key Words: Even-Odd-Mode Analysis, Microstrip Dual-Band BPF, Quarter-Wavelength Resonator, Transmission Zeros.

I. Introduction

In recent years, multiband bandpass filters (BPFs) have attracted considerable interest in modern fast-growing wireless communication technologies, such as GSM (global system for mobile communications), WLAN (wireless local area network) and RFID (radio-frequency identification) systems, because microwave filters are the key element to passing the desired electromagnetic signal and blocking the undesired frequency band signal. For this, multiband bandpass filters with excellent performance—such as high 3 dB roll-off skirts through the generation of transmission zeros (TZs) between the passbands—that are lightweight, low cost, compact size, and have high design flexibility are in strong demand [1–3].

To cope with the development of new era, dual-mode characteristics can be implemented using the step impedance technique, open-short-circuited stubs, substrate integrated waveguide (SIW), SIW with mushroom resonators, and quantic mode resonators [1–16]. For example, a dual-band filter centered at 2.4 GHz and 4 GHz based on a step impedance ring-loaded resonator is modelled in [1]. The presented filter shows a narrow bandwidth for the first passband and a wide bandwidth

Manuscript received December 27, 2020 ; Revised May 6, 2021 ; Accepted July 12, 2021. (ID No. 20201227-213J)
[1]Department of Electrical Engineering, University of Engineering and Technology, Peshawar, Pakistan.
[2]College of Engineering, Al-Ain University, UAE.
[3]Prince Sattam bin Abdulaziz University, Alkharj, Saudi Arabia.
[*]Corresponding Author: Abdul Basit (e-mail: abdulbasit@uetpeshawar.edu.pk)

for the second passband. A drawback of a larger circuit area and poor selectivity is seen by exciting only two TZs between the passbands. A selectivity enhancement method is introduced in [2] using step impedance resonator (SIR) to design a two-band filter; however, the structure fails to reduce insertion loss (IL) and increase fractional bandwidth (FBW), which degrades the overall performance. A low-cost and lightweight SIW-based first-order dual-band filter centered at 1.94 GHz and 4.84 GHz is designed in [3]. The presented structure has a compact circuit area, but greater in-band IL and poor sharpness are observed by introducing two TZs between the passbands. A dual-band filter for Wi-Fi and WLAN applications is modeled in [4] to overcome the drawbacks mentioned in [1–3]; however, the proposed design has a larger circuit area. A first-order dual-band filter with controllable bandwidth and wide stopband is designed in [5]. The filter shows a good FBW, but a complex larger circuit area and poor 3 dB roll-off skirts are the major drawbacks associated with the design. A hexagonal-shaped second-order dual-band filter with a simple topology is designed and fabricated in [6] based on a modified split ring resonator. The presented filter has good IL; however, a larger circuit dimension and poor selectivity degrade the filter performance by introducing two TZs in the passbands. A second-order filter centered at 2.25 GHz and 4.1 GHz is designed in [7], utilizing two mushroom resonators loaded inside in the cavity of SIW. However, the structure has the drawback of poor selectivity and larger circuit dimensions. To overcome the problems of poor sharpness and a larger circuit area in [5–7], a high selectivity first-order dual-band BPF based on the self-coupled resonator is designed in [8]. However, the proposed structure has the drawback of a narrow bandwidth and poor IL, especially in the second passband, which is greater than −3 dB. Second-order dual-band BPFs utilizing dual-mode dual loop resonators and multimode SIW cavity are reported in [9] and [10]. The proposed filters have good sharpness, but a narrow bandwidth, poor in-band ILs, and greater structural dimensions are the major problems related to these designs. A two-passband filter based on magnetically coupled resonators centered at 2.45 GHz and 5.6 GHz is designed and fabricated in [11]. However, the proposed structure has greater ILs and poor selectivity, consisting of only two TZs in the passband. Recently, high selectivity dual-band filters based on quantic-mode resonator and hairpin line resonators have been presented in [12] and [13]; however, the reported filters have poor ILs, narrow FBW, and larger structure size. The authors of [14] designed a second-order dual-band filter with controllable bandwidths at 2.1 GHz and 3.43 GHz based on a quintuple-mode resonator. The presented filter has the advantage of a wider bandwidth, but high IL, poor selectivity, and a larger circuit area are the drawbacks of this filter. A compact dual-band response for Wi-Fi and WLAN applications using SIR and shorted stub-loaded resonators was presented in [15]. The proposed filter has the advantage of high return loss and high selectivity by exciting five TZs near the passbands, but the drawbacks are a larger circuit dimension, a narrow bandwidth, and high in-band losses. Recently, a high selectivity dual-band response at 3.7 GHz and 4.8 GHz using the transversal signal interaction concept was designed in [16]. The proposed design shows good stopband performance by introducing a dozen TZs between 5.2 GHz and 40 GHz. However, the proposed filter has the drawback of high IL, narrow bandwidth in the first passband, and a larger circuit size.

This research designs a compact and lightweight dual-band filter for GSM and GPS (global positioning system) applications to overcome the above challenges. The presented structure is designed on a shorted T-shaped λ/4 resonator. A direct feed resonator provides the first passband and provides the source to load coupling for a higher frequency band internal resonator. The coupled resonators generate a pair of TZs in the passbands, which guarantees high-frequency selectivity. Resonators A and B are folded and connected to a metallic via to minimize the filter size. The key benefit of this design is that it controls all TZs without altering the central frequencies, which is later shown in the paper. A symmetrical arrangement was used to achieve the two passbands, i.e., 850 MHz and 1.57 GHz, using the method of even-odd-mode analysis. The filter was designed and tested for authentication to measure the level of matching between the experimental and measured data.

II. T-Shaped Resonator Analysis

In total, three stubs exist in the T-shaped resonator, in which two are open ended while the third one is short circuited and can be seen in Fig. 1, where Y_1 is admittance of the open-ended stubs with length L_1, and Y_2 is admittance of the short-ended stub with length L_2.

Since the topology obtained for this structure is symmetrical in nature with respect to plane A-A', an even-odd mode analysis will be performed for both resonators (i.e., A and B) for characterization of the two passbands. The corresponding circuits of the odd and even modes are depicted in Figs. 2 and 3. For the lower band, outer resonator A is directly fed to achieve source-to-load coupling for the inner one, which is B in our case and which is operating for the higher band. Therefore, the res-

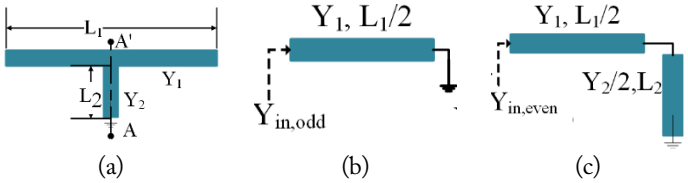

Fig. 1. Proposed T-shaped resonator (a) with equivalent odd mode (a) and even mode (c).

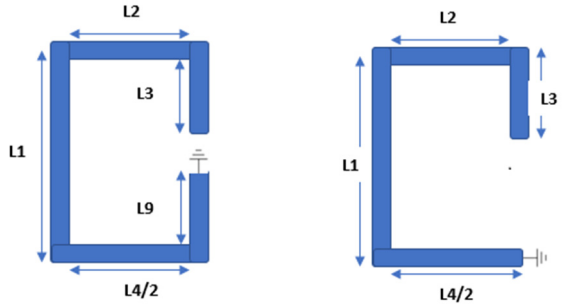

Fig. 2. (a) Odd-mode circuits and (b) even-mode circuits of resonator A.

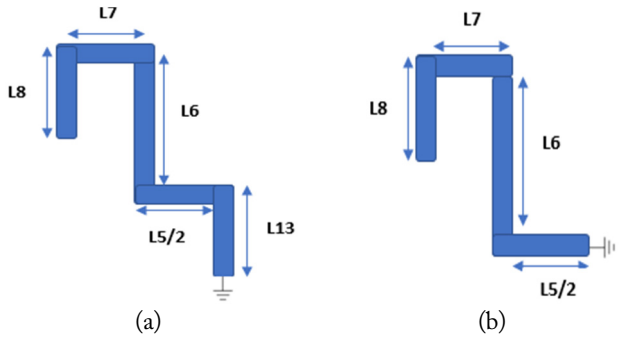

Fig. 3. (a) Odd-mode circuits and (b) even-mode circuits of resonator B.

onance frequency equations of the fundamental even and odd mode can be calculated using the procedure mentioned in [17] and [18] and is given as follows:

$$f_{even1} = \frac{(2n-1)c}{4(L_1 + L_2 + L_3 + L_{4/2} + L_9)\sqrt{\varepsilon_{eff}}} \quad (1)$$

$$f_{odd1} = \frac{(2n-1)c}{4(L_1 + L_2 + L_3 + L_{4/2})\sqrt{\varepsilon_{eff}}} \quad (2)$$

$$f_{even2} = \frac{(2n-1)c}{4(L_6 + L_7 + L_8 + L_{5/2} + L_{13})\sqrt{\varepsilon_{eff}}} \quad (3)$$

$$f_{odd2} = \frac{(2n-1)c}{4(L_6 + L_7 + L_8 + L_{5/2})\sqrt{\varepsilon_{eff}}} \quad (4)$$

In the above equations, c = 3 × 10^8 m/s and ε_{eff} show the effective permittivity of the substrate material. From Eqs. (1)–(4), the fundamental resonance frequencies can be obtained and are verified in Section IV.

III. Dual-Band Filter Geometry

Based on the geometrical study described in the previous section, a dual-band BPF, with a size of 22 × 21 mm^2 or 0.10 λ_g × 0.99 λ_g, is simulated in the High Frequency Structure Simulator (HFSS) 15 software, designed on the Rogers RO-4350 substrate having a height of 0.762 mm and relative permittivity of 3.66. The filter consists of two quarter-wavelength resonators with dual-mode symmetry. Both resonators are folded to minimize the circuit size. Fig. 4 illustrates the topology of the dual-band filter, and Table 1 sets out the geometric dimensions.

To evaluate the corresponding resonance frequencies of the dual-band filter, the physical length of each resonator is determined using an even-odd-mode method. The first passband is created by resonator A, which is used as the feed mechanism for the internal resonator B working at a higher band. As the dual band filter is based on a quarter wavelength resonator, there are two modes in each passband: one is even, and one is odd. The resonance frequency of the first even mode is 0.90 GHz and is found using Eq. (1) and Fig. 2(a). The fundamental odd-mode frequency (i.e., 0.86 GHz) is found using Eq. (2) and Fig. 2(b). Similarly, Eqs. (3)–(4) and Fig. 3(c)–3(d) are utilized for the even-odd resonant frequencies of the second passband, i.e., f_{even} = 1.53 GHz and f_{odd} = 1.57 GHz. The slight difference in frequencies is due to the resonator coupling, and they are adjusted in the HFSS software to our desired band applications.

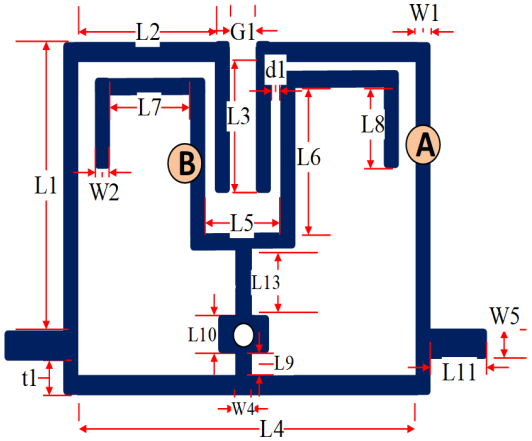

Fig. 4. Proposed dual-band BPF topology.

Table 1. Geometrical length of the proposed dual-band BPF (unit: mm)

Parameter	Value	Parameter	Value
L_1	18.6	L_{10}	1
L_2	7	L_{11}	3
L_3	12	W_1	1.7
L_4	18.6	W_2	0.6
L_5	6.3	W_4	0.5
L_6	11	r	0.2
L_7	5.2	G_1	1.2
L_8	1	t_1	0.7
L_9	1.5	d_1	0.25

As seen in Fig. 5(a), length L_3 is the controlling parameter of the first passband, and by altering, only the first passband is shifted while the second passband is unaffected. Similarly, in Fig. 5(b), length L_6 controls the second passband, and by changing, it will shift only the second band while keeping the first band fixed. Thus, it is confirmed that the proposed filter is capable of independently controlling the two passbands.

The second advantage of the proposed filter is that the transmission zeros on either side of the passbands can be regulated according to the appropriate stopband frequency. As shown in Fig. 6, only the position of TZs is influenced by changing parameter t_1, while the central frequencies remain fixed. This property makes the proposed filter unique compared to other published dual-band BPFs in the existing literature. We generate four transmitting zeros in the following manner. TZ_1 is produced through source-to-load coupling, TZ_3 is the inherent transmission zero, and TZ_2 and TZ_4 are excited with the help of two coupled symmetrical open-ended stubs.

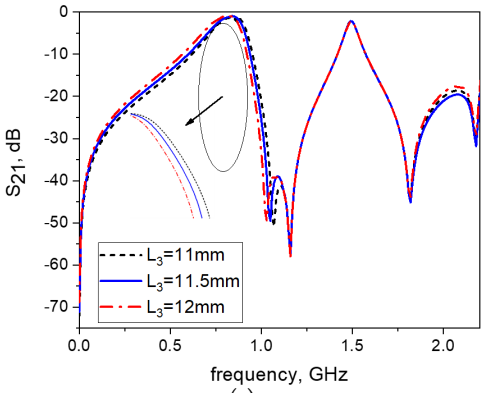

Fig. 5. Control of the first band (a) and second band (b) of the proposed dual-band filter.

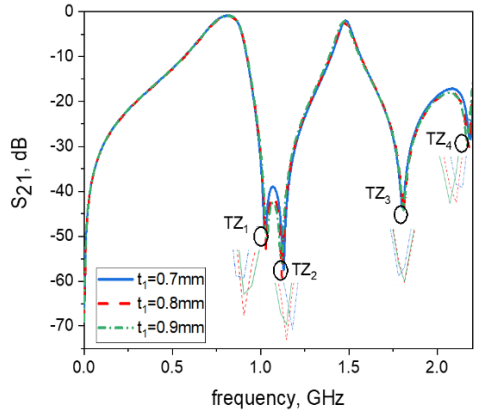

Fig. 6. Control of transmission zeros against parameter t_1.

The coupling coefficient (K_e) and external quality factor (Q_{ext}) is determined using the following equations [18–22];

$$K_e = \frac{f_2^2 - f_1^2}{f_2^2 + f_1^2}, \tag{5}$$

$$Q_{ext} = \frac{f_c}{B.W_{3dB}}. \tag{6}$$

In Eqs. (5) and (6), K_e denotes the coupling coefficient, Q_{ext} represents the external quality factor, f_2 and f_1 represent the higher and lower frequencies of each passband, f_c is the central resonance frequency, and $B.W_{3dB}$ is the absolute bandwidth at central frequency. K_e can be determined by the coupling between the two resonators, while Q_{ext} could be measured according to the outer resonator and the feedlines. As shown in Figs. 7 and 8, the coupling coefficient decreases as gap G_1 and d_1 increases with an increasing external quality factor [16, 17, 23]. Fig. 9 indicates the relationship between Q_{ext} and

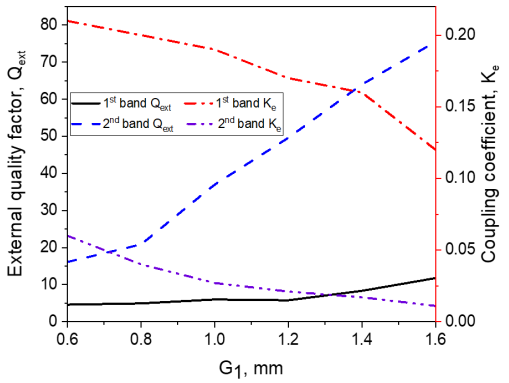

Fig. 7. Effect of K_e and Q_{ext} with respect to parameter G_1.

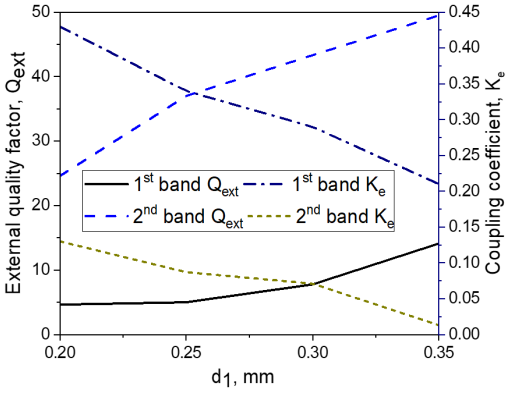

Fig. 8. Effect of K_e and Q_{ext} with respect to parameter d_1.

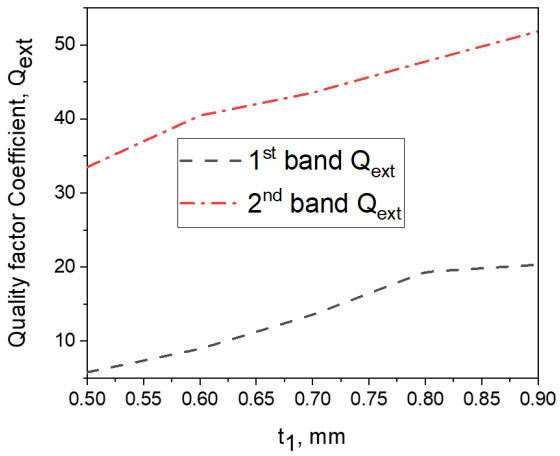

Fig. 9. External quality factor against parameter t_1.

parameter t_1, and by increasing t_1, Q_{ext} also increases according to Eq. (5). Figs. 7 and 8 present graphical plots of Q_{ext} and Ke with respect to parameters G_1 and d_1. The figures show that if gap G_1 increases, K_e decreases accordingly, while Q_{ext} improves in Eqs. (5) and (6).

IV. Experimental and Measured Results

The proposed technique has been simulated and tested for a compact dual-band BPF. The filter is modelled in the following way. First, the sample is designed in the ANSYS HFSS 15 electromagnetic simulator, and parametric analysis is performed to obtain the required dual-band frequencies. The simulated model is then checked for authentication using the Agilent E5071C network analyzer. In Fig. 10, a significant match can be found between the experimental and fabricated results. For feeding, two 50-Ω feedlines of 1.7 mm width are connected on both sides of the filter. The filter consists of two resonators A and B to control both bands separately. The first operational band is generated by resonator A, which provides the load-to-source coupling for the second resonator, which creates the second passband. For wireless applications such as GSM and GPS, the presented dual-band filter resonates at fundamental frequencies, i.e., 850 MHz and 1.57 GHz. The absolute bandwidth for each passband was 16.84% and 3.5%. A return loss of more than −15 dB was seen for each passband. Four controllable TZs were excited at different frequencies (i.e., 1.04 GHz, 1.16 GHz, 1.82 GHz, and 2.22 GHz) to increase the sharpness and the stop band performance of the filter. For the GSM and GPS frequency bands, the minimum ILs ($-20\log|S_{21}|$) are 0.98 dB and 1.11 dB, respectively. Moreover, Table 2 provides a detailed comparison datasheet with the most recent published work in terms of IL, FBW, TZs, and circuit area [3–14]. The comparison shows that the presented structure has the potential to compete in the market with existing ones for wireless applications.

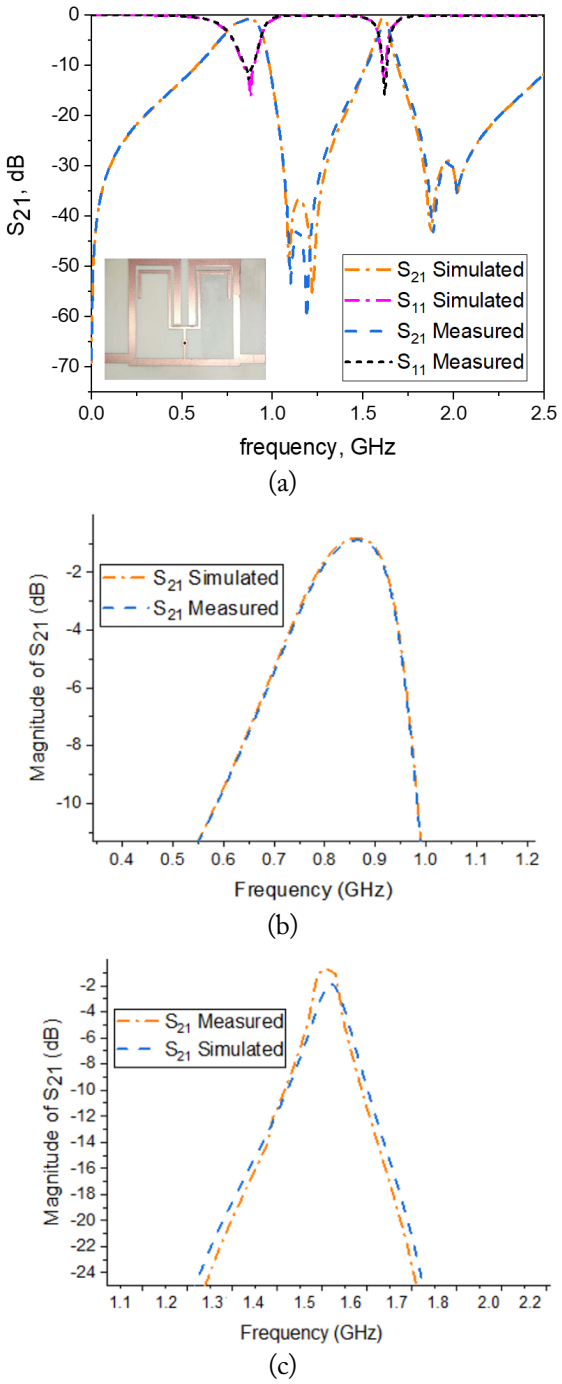

Fig. 10. (a) Experimental and measured frequency plots of the proposed dual-band filter. (b) First passband in detail. (c) Second passband in detail.

V. Conclusion

In this article, a symmetric T-shaped dual-mode λ/4 resonator is employed for designing a compact dual passband filter for wireless applications such as GSM and GPS systems. The dual-band filter with four controllable transmitting zeros was obtained using λ/4 wavelength (A and B) resonators. The fabricated filter has a total size of 22 × 21 mm² independent of the feed-

Table 2. Comparison with published dual-passband designs

Study	CF (GHz)	IL (dB)	3-dB FBW (%)	Circuit size ($\lambda_g \times \lambda_g$)	TZs	Filter order
Yin and Lin [3]	1.94 / 4.85	1.26 / 2.69	14.43 / 2.69	0.179 × 0.097	2	2
Xu et al. [5]	2.57 / 3.41	1.01 / 1.33	21.05 / 16.4	0.62 × 0.31	3	2
Troudi et al. [6]	2.5 / 4.83	0.45 / 0.6	18 / 8	142.6 mm^2	2	2
Chaudhury et al. [7]	2.25 / 4.1	0.86 / 1.6	12.9 / 10.8	0.26 × 0.43	3	2
Wang et al. [8]	2.02 / 3.03	2.4 / 3.6	8.4 / 6.3	0.16 × 0.23	6	2
Liu et al. [9]	3.25 / 3.75	1.88 / 2.15	3.17 / 2.1	0.22 × 0.22	3	2
Yang et al. [10]	6.95 / 7.95	1.47 / 1.65	2.6 / 2.3	2.2 × 0.61	4	2
Fernandez-Prieto et al. [11]	2.3 / 3.2	1.1 / 1.7	11.3 / 9.4	0.228 λ_g^2	4	2
Li et al. [12]	2.38 / 4.98	2.2 / 1.6	8 / 8.8	0.18 × 0.20	4	2
Chang et al. [13]	2.44 / 5.57	2.78 / 2.85	NA	0.029	2	1
Zhang et al. [14]	2.1 / 3.43	1.4 / 1.9	17.1 / 12.2	0.19 × 0.21	2	2
Zhou et al. [15]	2.4 / 5.2	1.2 / 2	8 / 5	100.1 mm^2	4	2
Wang et al. [16]	3.8 / 4.8	1.38 / 1.82	11.3 / 10.7	0.16 × 0.31	>13	2
This work	0.85 / 1.57	0.98 / 1.11	16.84 / 3.5	0.10 × 0.09	4	1

Values of CF, IL, and FBW are presented as first passband / second passband.

line. Finally, the filter has been fabricated to check the simulated results with the measured one. Owing to the planar structure, low losses, and compact size, the designed filter has good integration ability in the existing emerging wireless multiband applications.

REFERENCES

[1] M. H. Weng, S. W. Lan, S. J. Chang, and P. Y. Yang, "Design of dual-band bandpass filter with simultaneous narrow-and wide-bandwidth and a wide stopband," *IEEE Access*, vol. 7, pp. 147694-147703, 2019.

[2] R. Gomez-Garcia, L. Yang, J. M. Munoz-Ferreras, and D. Psychogiou, "Selectivity-enhancement technique for stepped-impedance-resonator dual-passband filters," *IEEE Microwave and Wireless Components Letters*, vol. 29, no. 7, pp. 453-455, 2019.

[3] B. Yin and Z. Lin, "A novel dual-band bandpass SIW filter loaded with modified dual-CSRRs and Z-shaped slot," *AEU-International Journal of Electronics and Communications*, vol. 121, article no. 153261, 2020. https://doi.org/10.1016/j.aeue.2020.153261

[4] G. Z. Liang and F. C. Chen, "A compact dual-wideband bandpass filter based on open-/short-circuited stubs," *IEEE Access*, vol. 8, pp. 20488-20492, 2020.

[5] L. Xu, H. J. Yue, F. Wei, and X. W. Shi, "A balanced dual-band bandpass filter with a wide stopband and controllable differential-mode frequencies and fractional bandwidths," *International Journal of RF and Microwave Computer-Aided Engineering*, vol. 30, no. 1, article no. e22013, 2020. https://doi.org/10.1002/mmce.22013

[6] Z. Troudi, J. Machac, and L. Osman, "Compact dual-band bandpass filter using a modified hexagonal split ring resonator," *Microwave and Optical Technology Letters*, vol. 62, no. 5, pp. 1893-1899, 2020.

[7] S. S. Chaudhury, S. Awasthi, and R. K. Singh, "Dual band bandpass filter based on substrate integrated waveguide loaded with mushroom resonators," *Microwave and Optical Technology Letters*, vol. 62, no. 6, pp. 2226-2235, 2020.

[8] X. Wang, J. Wang, L. Zhu, W. W. Choi, and W. Wu, "Compact stripline dual-band bandpass filters with controllable frequency ratio and high selectivity based on self-coupled resonator," *IEEE Transactions on Microwave Theory and Techniques*, vol. 68, no. 1, pp. 102-110, 2020.

[9] Q. Liu, D. Zhang, J. Zhang, D. Zhou, and N. An, "Compact single-and dual-band bandpass filters with controllable transmission zeros using dual-layer dual-mode loop resonators," *IET Microwaves, Antennas & Propagation*, vol. 14, no. 6, pp. 522-531, 2020.

[10] Z. Yang, B. You, and G. Luo, "Dual–/tri-band bandpass filter using multimode rectangular SIW cavity," *Microwave and Optical Technology Letters*, vol. 62, no. 3, pp. 1098-1102, 2020.

[11] A. Fernandez-Prieto, J. Martel, P. J. Ugarte-Parrado, A. Lujambio, A. J. Martinez-Ros, F. Martin, F. Medina, and R. R. Boix, "Compact balanced dual-band bandpass filter

with magnetically coupled embedded resonators," *IET Microwaves, Antennas & Propagation*, vol. 13, no. 4, pp. 492-497, 2019.

[12] K. Li, G. Q. Kang, H. Liu, and Z. Y. Zhao, "High-selectivity adjustable dual-band bandpass filter using a quantic-mode resonator," *Microsystem Technologies*, vol. 26, no. 3, pp. 913-916, 2020.

[13] H. Chang, W. Sheng, J. Cui, and J. Lu, "Multilayer dual-band bandpass filter with multiple transmission zeros using discriminating coupling," *IEEE Microwave and Wireless Components Letters*, vol. 30, no. 7, pp. 645-648, 2020.

[14] S. F. Zhang, L. T. Wang, S. H. Zhao, J. Zhou, Z. P. Wang, X. Zhang, X. L. Liang, M. He, and L. Ji, "Design of dual-/tri-band BPF with controllable bandwidth based on a quintuple-mode resonator," *Progress in Electromagnetics Research Letters*, vol. 82, pp. 129-137, 2019.

[15] M. Zhou, X. Tang, and F. Xiao, "Compact dual band transversal bandpass filter with multiple transmission zeros and controllable bandwidths," *IEEE Microwave and Wireless Components Letters*, vol. 19, no. 6, pp. 347-349, 2009.

[16] L. T. Wang, Y. Xiong, L. Gong, M. Zhang, H. Li, and X. J. Zhao, "Design of dual-band bandpass filter with multiple transmission zeros using transversal signal interaction concepts," *IEEE Microwave and Wireless Components Letters*, vol. 29, no. 1, pp. 32-34, 2018.

[17] D. M. Pozar, *Microwave Engineering*. Hoboken, NJ: John Wiley & Sons, 2009.

[18] A. Basit and M. I. Khattak, "Designing modern compact microstrip planar quadband bandpass filter for hand held wireless applications," *Frequenz*, vol. 74, no. 5-6, pp. 219-227, 2020.

[19] R. Kumar and S. N. Singh, "Design and analysis of ridge substrate integrated waveguide bandpass filter with octagonal complementary split ring resonator for suppression of higher order harmonics," *Progress in Electromagnetics Research C*, vol. 89, pp. 87-99, 2019.

[20] A. K. Gorur, "A novel compact microstrip balun bandpass filter design using interdigital capacitor loaded open loop resonators," *Progress in Electromagnetics Research Letters*, vol. 76, pp. 47-53, 2018.

[21] F. Wei, H. J. Yue, X. H. Zhang, and X. W. Shi, "A balanced quad-band BPF with independently controllable frequencies and high selectivity," *IEEE Access*, vol. 7, pp. 110316-110322, 2019.

[22] Q. Yang, Y. C. Jiao, and Z. Zhang, "Compact multiband bandpass filter using low-pass filter combined with open stub-loaded shorted stub," *IEEE Transactions on Microwave Theory and Techniques*, vol. 66, no. 4, pp. 1926-1938, 2018.

[23] A. Basit and M. I. Khattak, "Design and analysis of a microstrip planar UWB bandpass filter with triple notch bands for WiMAX, WLAN, and X-Band satellite communication systems," *Progress in Electromagnetics Research M*, vol. 93, pp. 155-164, 2020.

Abdul Basit

received a B.Sc. degree in electrical engineering in 2012 from the University of Engineering and Technology Peshawar, Pakistan, an MSc. degree in 2013 from the CECOS University of IT and Emerging Sciences, Peshawar, Pakistan, and a Ph.D. degree in electrical engineering from the University of Engineering and Technology Peshawar, Pakistan, in 2021 under the supervision of Dr. Muhammad Irfan Khattak with a specialization in microwave filters. From 2013 to 2017, he was a lecturer in the electrical engineering department University of Engineering and Technology Bannu Campus, Pakistan. From 2017 to 2018, he served as an Assistant Director (Technical) at the National Transmission and Dispatch Company (NTDC). He is now working as a lecturer in the Electrical Engineering Department, University of Engineering and Technology, Peshawar, Pakistan.

Muhammad Irfan Khattak

works as an associate professor in the Department of Electrical Engineering at the University of Engineering and Technology, Peshawar. He received his B.Sc. in electrical engineering from the same university in 2004 and his Ph.D. from Loughborough University, UK, in 2010. After completing his Ph.D., he was appointed chairman of the Electrical Engineering Department at the University of Engineering & Technology Bannu Campus for 5 years and managed academic and research activities in this department. Later, in 2016, he was appointed the campus coordinator of the UET Kohat Campus and took over administrative control. He also heads a research group called the Microwave and Antenna Research Group, where he supervises postgrad students working on the latest trends in antenna technology, such as 5G and graphene nano-antennas for THz, opto-electronic, and plasmonic applications. His research interests include antenna design, on-body communications, anechoic chamber characterization, speech processing, and speech enhancement. Besides his research activities, he is a certified OBE outcome based education (expert with the PEC Pakistan Engineering Council) for organizing OBA-based accreditation visits.

Muath Al-Hasan

received a B.Sc. degree in electrical engineering from the Jordan University of Science and Technology, Jordan, in 2005, an M.Sc. in wireless communications from Yarmouk University, Jordan, in 2008, and a Ph.D. in telecommunication engineering from Institut National de la Recherche Scientifique (INRS), Université du Québec, Canada, 2015. From 2013 to 2014, he worked with Planets Inc., in California, USA. In May 2015, he joined Concordia University in Canada on a postdoctoral fellowship. He is currently an assistant professor at Al Ain University in the United Arab Emirates. His current research interests include antenna design at millimeter-wave and terahertz, and machine learning and artificial intelligence in antenna design.

Jamel Nebhen

received an M.Sc. from the National Engineering School of Sfax, Tunisia, in 2007, and a Ph.D. degree from Aix-Marseille University, France, in 2012, both in microelectronics. From 2012 to 2018, he worked as a postdoctoral researcher in France at LIRMM-Lab Montpellier, IM2NP-Lab Marseille, ISEP Paris, LE2I-Lab Dijon, Lab-Sticc Telecom Bretagne Brest, and IEMN-Lab Lille. Since 2019, he has joined Prince Sattam bin Abdulaziz University in Alkharj, Saudi Arabia, as an assistant professor. His research interests are mainly in the design of analog and RF integrated circuits, IoT, biomedical circuits, and sensor instrumentation.

Atif Jan

obtained his B.Sc. degree in Electrical Engineering from University of Engineering and Technology (UET), Peshawar in 2011 and M.Sc. degree in Electrical Engineering from UET, Peshawar in 2015. He is working as a lecturer at the Department of Electrical Engineering, UET Peshawar since 2013. He is a Ph.D. scholar, and his research interests include image processing, computer vision, machine learning and deep learning.